Bioresource Technology 297 (2020) 122520

Contents lists available at ScienceDirect

Bioresource Technology

journal homepage: www.elsevier.com/locate/biortech

Kinetic modeling of anaerobic carboxylic acid production from swine wastewater

Naassom Wagner Sales Morais[a], Milena Maciel Holanda Coelho[a], Amanda de Sousa e Silva[a], Erlon Lopes Pereira[a], Renato Carrhá Leitão[b], André Bezerra dos Santos[a,*]

[a] Department of Hydraulic and Environmental Engineering, Federal University of Ceará, Fortaleza, Ceará, Brazil
[b] Embrapa Agroindústria Tropical. Rua Dra. Sara Mesquita, 2270, Zip: 60511-110, Fortaleza, CE, Brazil

GRAPHICAL ABSTRACT

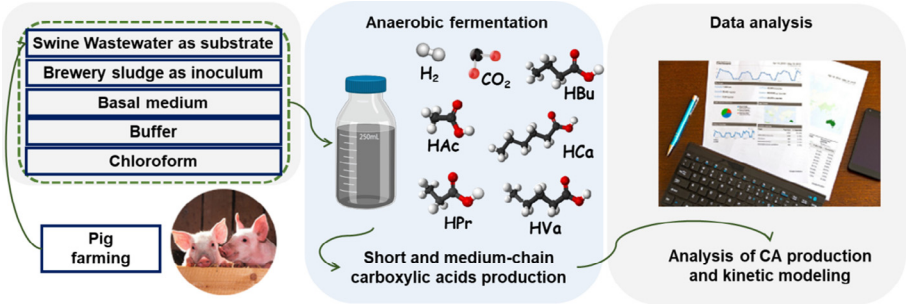

ARTICLE INFO

Keywords:
Resource recovery
Carboxylic platform
Agroindustrial waste
Swine wastewater
Kinetic modeling

ABSTRACT

This work aimed to evaluate the potential of anaerobic carboxylic acids (CA) production from swine wastewater (SW), perform modeling studies of the acidogenic process and estimate the kinetic parameters. Tests were carried out in four batch reactors with 250 mL reaction volume, with brewery sludge as inoculum and using chloroform (0.05%, v/v) for methanogenesis inhibition. Hydrolysis was the main limiting step of CA production from SW, once that it took more than twenty days for the particulate COD consumption to stabilize and fourteen days to produce 60% of the acids formed. A yield of 0.33 mg $mgCOD_A^{-1}$, corresponding to 0.40 mgCOD $mgCOD_A^{-1}$, was obtained. Kinetic models describing logistic growth functions were best suited to simulate CA production.

1. Introduction

Pork is the most consumed meat in the world (Cheng et al., 2019). In 2018, it is estimated that the worlds pork production was 120.5 million tons, an increase of 0.65% over 2017 (FAO, 2019). However, such a demand results in severe environmental impacts, such as high volumes of swine wastewater (SW), and greenhouse gas (GHG) emissions, in which 9% of the GHG emissions from livestock come from pig farming (Cheng et al., 2019; Groen et al., 2016). Studies indicate that about 4–8 L of SW are generated daily per swine (García et al., 2017; Nagarajan et al., 2019).

SW are wastes composed of wasted feed, water spilled from drinking fountains, animal excrement, water used for cleaning and sanitizing the farms. This kind of wastewater has high levels of organic matter, suspended solids, nutrients, and considerable microbial load, besides residues of antibiotics and hormones extensively used to improve pig

* Corresponding author at: Department of Hydraulic and Environmental Engineering, Campus do Pici, Bloco 713. Pici. CEP: 60455-900, Fortaleza, Ceará, Brazil.
E-mail address: andre23@ufc.br (A.B. dos Santos).

https://doi.org/10.1016/j.biortech.2019.122520
Received 30 September 2019; Received in revised form 25 November 2019; Accepted 27 November 2019
Available online 29 November 2019
0960-8524/

productivity, especially in developed countries (Xu et al., 2019). Thus, if the SW are improperly disposed, it can cause many different environmental impacts such as eutrophication, soil and water pollution, bacterial resistance to antibiotics, among others (Cheng et al., 2018). On the other hand, such SW can be used for production of methane (Yang et al., 2016), hydrogen (Wagner et al., 2009), fertilizer (Huang et al., 2016; Kwon et al., 2018), and other high added-value products, for instance, carboxylic acids (CA).

Short-chain carboxylic acids (SCCAs) are the main products of acidogenic fermentation of macromolecules. These compounds can be applied as a renewable carbon source for the production of building block chemicals in the food, pharmaceutical and chemical industries (Atasoy et al., 2018). In addition, through the Biological Carboxylic Chain Elongated Process (BCCEP), SCCAs can be bioconverted to medium-chain carboxylic acids (MCCAs), which have higher market value than SCCAs due to their nobler purposes, such as in production of bioplastics and biodiesel, as well as ease of extraction from the fermentative medium due to increased hydrophobicity of the molecules (Fang et al., 2020; Han et al., 2019). However, the elongation process depends on several operational parameters for imposing the strict metabolic pathway, which is still not completely clear.

One of the alternatives to improve the understanding of the acidogenic process is the use of mathematical models. Mathematical modeling is a widely used tool for predicting bioreactor performance, assisting in pilot plant studies by providing design and operation data, leading to greater process efficiency and less dependence on qualified operators (Membere and Salles, 2018). Moreover, mathematical modeling is able to provide kinetic parameter estimation and process simulation, essential tools for designing, operating and optimizing biological treatment plants, as minor improvements in systems can generate significant economic returns (Ebrahimi et al., 2018). A diversity of kinetic parameters can be estimated from kinetic modelings, such as first-order production rate constant (k), maximum microbial growth rate (μ_{max}), lag phase time (λ) and the maximum production rate of the bioproduct of interest (Sun et al., 2015).

Although SW treatment is widely investigated in terms of methane and nutrients recovery (Kwon et al., 2018; Huang et al., 2017), microalgae cultivation (Leite et al., 2019), among others, the application of SW from the perspective of the carboxylic platform is still incipient in the literature. Moreover, there are a few studies of modeling applied to methanogenic-inhibited systems. This work aimed to evaluate the potential of anaerobic CA production from swine wastewater, perform modeling studies of the acidogenic process and estimate the kinetic parameters.

2. Materials and methods

2.1. Inoculum and substrate

SW was obtained from a pig farm located at Chorozinho, Ceará, Brazil. The batch reactors used in the carboxylic acid production potential (CAPP) assays were inoculated with methanogenic sludge from an upflow anaerobic sludge blanket reactor (UASB) treating brewery wastewater (Dams et al., 2018). The concentrations of total solids (TS), total volatile solids (TVS) and total fixed solids (TFS) were 81.0, 33.8, 47.2 g L^{-1}, respectively.

The values of the physical–chemical parameters of the SW used in this experiment are in agreement with other investigations (Cheng, et al., 2018; Ding et al., 2017; Huang et al., 2016). The physical–chemical characterization analyses were performed according to Standard Methods for the Examination of Water and Wastewater (APHA, 2012).

2.2. Carboxylic acids production potential assays

The CAPP assays were performed in four borosilicate batch reactors, with 300 mL total volume, 250 mL reactional volume and 50 mL headspace. The basal medium and buffering at pH 7.0, previously adjusted with 1 M HCl or NaOH, were performed according to Dams et al. (2018). The food/microorganism (F/M) ratio was 0.64 ± 0.01 gCOD·gVSS^{-1}. To inhibit the methanogenic activity, 0.05% (v/v) chloroform was added (Viana et al., 2019). The reactors were sealed with rubber stoppers and purged with nitrogen (N_2) for 1 min in order to create an anaerobic atmosphere. They were then kept in an incubator under orbital shaking at 150 rpm and at 35 °C for 28 days (Jiang et al., 2013; Yin et al., 2017).

Samples were collected from the reactors on days 0, 2, 4, 7, 14, 21 and 28 for the analysis of chemical oxygen demand (COD) and quantification of the formed CA. At the end of the experiment (28th day), a gas sample was extracted from the headspace of the reactors to verify the inhibition of methanogenic activity and to determine the average concentrations of CH_4, H_2, CO_2 and H_2S present in the biogas.

Table 1
Equations used in calculating the organic matter fractions.

Equation	Number
$COD_P = COD_T - COD_S$	1
$COD_A = COD_T - COD_{CA(t0)}$	2
$COD_{Bio} = COD_S - COD_{CA}$	3
$COD_{CA} = COD_{CA(tf)} - COD_{CA(t0)}$	4
$Y1_{AC} = \frac{COD_{CA}}{COD_A}$	5
$Y2_{AC} = \frac{M_{CA}}{M_{TCA}}$	6
Selectivity $= \frac{M_{CA}}{M_{TCA}} x100$	7
Productivity $= \frac{C_{CA1D} - C_{CAB}}{Time}$	8

COD_P: particulate COD added in the batch reactor; COD_T: total COD added in the batch reactor; COD_S: soluble COD added in the batch reactor; COD_A: the fraction of the total COD available to be bioconverted to CA or directed to cell growth and biogas formation, corresponds to the total COD fraction applied at the beginning of the experiment that is not in the form of CA; $COD_{CA\ (T0)}$: the fraction of soluble COD in the form of CA at the beginning of the batch; COD_{BIO}: fraction of COD soluble not referring to CA; COD_{CA}: mass of CA formed during the incubation period; $COD_{CA\ (TF)}$: mass of CA at the end of the incubation period; $Y1_{CA}$: stoichiometric coefficient of COD yield converted to CA; $Y2_{CA}$: acid production in relation to the available COD (mg acids $gCOD_A^{-1}$); M_{CA}: mass of carboxylic acid formed during the incubation period (mg acid); M_{TCA}: total mass of carboxylic acids formed during the incubation period (mg acid); Selectivity: percentage of each acid formed in relation to the total acids produced (%); Productivity: quantity of acid present per working volume and per time (mg acid $L^{-1}\cdot d^{-1}$); C_{CA1D}: acid concentration at one day of collection (mg acid L^{-1}); C_{CAB}: acid concentration at the beginning of the batch (day zero) (mg acid L^{-1}) and Time: unit of time (d). Units in mgCOD.

2.3. Analytical methods

The biogas composition was analyzed by gas chromatography-barrier ionization discharge (GC BID-2010 Plus, Shimadzu Corporation, Japan) equipped with GS GASPRO column (60 m × 0.32 mm) (Agilent Technologies Inc., USA). The temperatures of oven, injector and detector were 250, 50 and 100 °C, respectively. Helium gas was used as carrier gas in a flow of 2 mL min^{-1}, and the run time of the method was 9 min. After the gas chromatography analysis, the cumulative biogas volume in the headspace was measured from the displacement of a saline solution (NaCl 25 g·L^{-1}) acidified to pH 2.0 with sulfuric acid (H_2SO_4) P.A. in a Mariotte bottle.

Acetic (HAc), propionic (HPr), butyric (HBu), isovaleric (HIVa), valeric (HVa) and caproic (HCa) acids concentrations were determined by high performance liquid chromatography (HPLC) (LC-20A,

Table 2
Models selected to describe the bioconversion of organic matter.

Kinetic Model	Equation of the Kinetic Model
Hydrolysis of Particulate Organic Matter	
First-order	$C_t = C_0 exp(-kt)$
First-order with Residual	$C_t = C_r + (C_0 - C_r) exp(-kt)$
Consumption of Biodegradable Organic Matter (Biodegradable COD)	
First-order	$C_t = C_0 exp(-kt)$
First-order with Residual	$C_t = C_r + (C_0 - C_r) exp(-kt)$
Logistic	$C_t = \frac{C_0 + X_0}{1 + (X_0 / C_0) exp[K_L (C_0 + X_0) t]}$ $K_L = \frac{\mu_{máx}}{K_s}$ $\quad K_B = K_L \times X_0$
Monod with Growth	$C_t = exp\left(\frac{(C_0 + X_0 + K_S)\ln\left(\frac{X}{X_0}\right) - (C_0 + X_0)\mu_{máx} t + K_S \ln(C_0)}{K_s}\right)$
Production of Carboxylic Acids	
First-order	$CA_t = CA_f [1 - exp(-k_{CA} t)]$
Second-order	$CA_t = \frac{k_{CA}''(CA_f)^2 t}{1 + k_{CA}''(CA_f) t}$
Fitzhugh	$CA_t = CA_f [1 - exp(-k_{CA} t)^n]$
Monomolecular	$CA_t = CA_f [1 - \exp(-K_{CA}(t - \lambda))]$
Modified Gompertz	$CA_t = CA exp\left\{-exp\left[\frac{\mu_m e}{CA_f}(\lambda - t) + 1\right]\right\}$
Logistic	$CA_t = \frac{CA_f}{1 + exp\left[\frac{4\mu_m(\lambda - t)}{CA_f} + 2\right]}$
Transference	$CA_t = CA_f \left\{1 - exp\left[-\frac{\mu_m (t - \lambda)}{CA_f}\right]\right\}$
Richards	$CA_t = CA_f \left\{1 + v.\ exp(1 + v).\ exp\left[\frac{\mu_m}{CA_f}.\ (1 + v)\left(1 + \frac{1}{v}\right)(\lambda - t)\right]\right\}^{(-1/v)}$

C_t: concentration of organic matter over time; C_0: initial organic matter concentration; k: velocity constant (k_H: hydrolysis rate constant/k_B: soluble substrate degradation rate constant); C_r: residual organic matter concentration; X_0: initial biomass concentration; X: final biomass concentration; k_L: Logistic model constant; K_S: saturation constant/Monod constant; μ_{max}: maximum microbial growth rate; CA_t: CA concentration over time; CA_f: final concentration of CA; k_{CA}: first-order CA production rate constant, k_{CA}": second-order CA production rate constant, t: digestion time, n: shape constant; e: Euler number; λ: lag phase time; μ_m: maximum CA productivity.

Table 3
Selectivity, yields, final concentration and maximum productivity of carboxylic acids.

Parameter	HAc	[f]HPr	HBu	HIVa	HVa	HCa
[a]Final Concentration	795 ± 59	86 ± 34	136 ± 7	62 ± 4	19 ± 2	49 ± 5
[b]$Y1_{CA}$	341 ± 25	–	99 ± 5	51 ± 3	15 ± 2	43 ± 5
[c]$Y2_{CA}$	320 ± 24	–	55 ± 3	25 ± 2	8 ± 1	20 ± 2
[d]Maximum productivity	101 ± 46	–	16 ± 9	10 ± 3	1 ± 0	2 ± 0
[e]Selectivity	75 ± 1	–	13 ± 1	6 ± 0	2 ± 0	4 ± 0

a) Final concentration of carboxylic acids at the end of the experiment (mg L^{-1}); b) The production yield of COD_{CA} in relation to the available COD ($mgCOD_{CA}$ $gCOD_A^{-1}$); c) The production yield of acids in relation to the available COD (mg acids $gCOD_A^{-1}$); d) Maximum productivity of acids (mg acids L^{-1} d^{-1}); e) Percentage of a specific acid in relation to the total acids produced (%); f) Production yields for HPr were not considered because HPr consumption exceeded its production during batch testing. However, its residual concentration was considered for calculations of total CA production yield ($Y1_{CA}$ and $Y2_{CA}$).

Prominence, Shimadzu Corporation, Japan) equipped with an Aminex HPX-87H column (300 mm × 7.8 mm) (Bio-Rad, USA), at 65 °C, with 5 mM H_2SO_4 in deionized water as eluent (isocratic flow of 0.6 mL·min^{-1}) and refractive index detector (RID-10A, Shimadzu Corporation, Japan). For the chromatographic and soluble COD analyzes, the samples were filtered on 0.45 μm pore glass fiber membrane.

2.4. Organic matter fractions and yields

Organic matter fractions and yields were calculated using Eq. (1 to 8) expressed in Table 1. The concentration of organic matter (COD in the form of acids) of each acid was obtained by the following conversion factors: 1 mg HAc = 1.07 mgCOD. 1 mg HPr = 1.51 mgCOD. 1 mg HBu = 1.82 mgCOD. 1 mg HIVa = 2.04 mgCOD. 1 mg HVa = 2.04 mgCOD. 1 mg HCa = 2.21 mgCOD (Moscoviz et al., 2018).

2.5. Kinetic study on CAPP assays

The equations of the kinetic models selected to describe the bioconversion of organic matter and the production of CA are presented in Table 2. A nonlinear least-squares regression analysis was performed using the Microsoft Office Excel 2019 Solver tool to estimate the parameters of the selected kinetic models (Lima et al., 2018). Data obtained from kinetic modeling was applied to plot the curves of each process using Origin software version 8.1 (OriginLab Corporation, Northampton, MA, USA).

The selection of the model that best describes each organic matter bioconversion process was performed using the coefficient of determination (R^2) and the Akaike Information Criterion (AIC). The lower the value of the AIC, the greater the adequacy of the data estimated by the kinetic model to the experimental data. The AIC was calculated

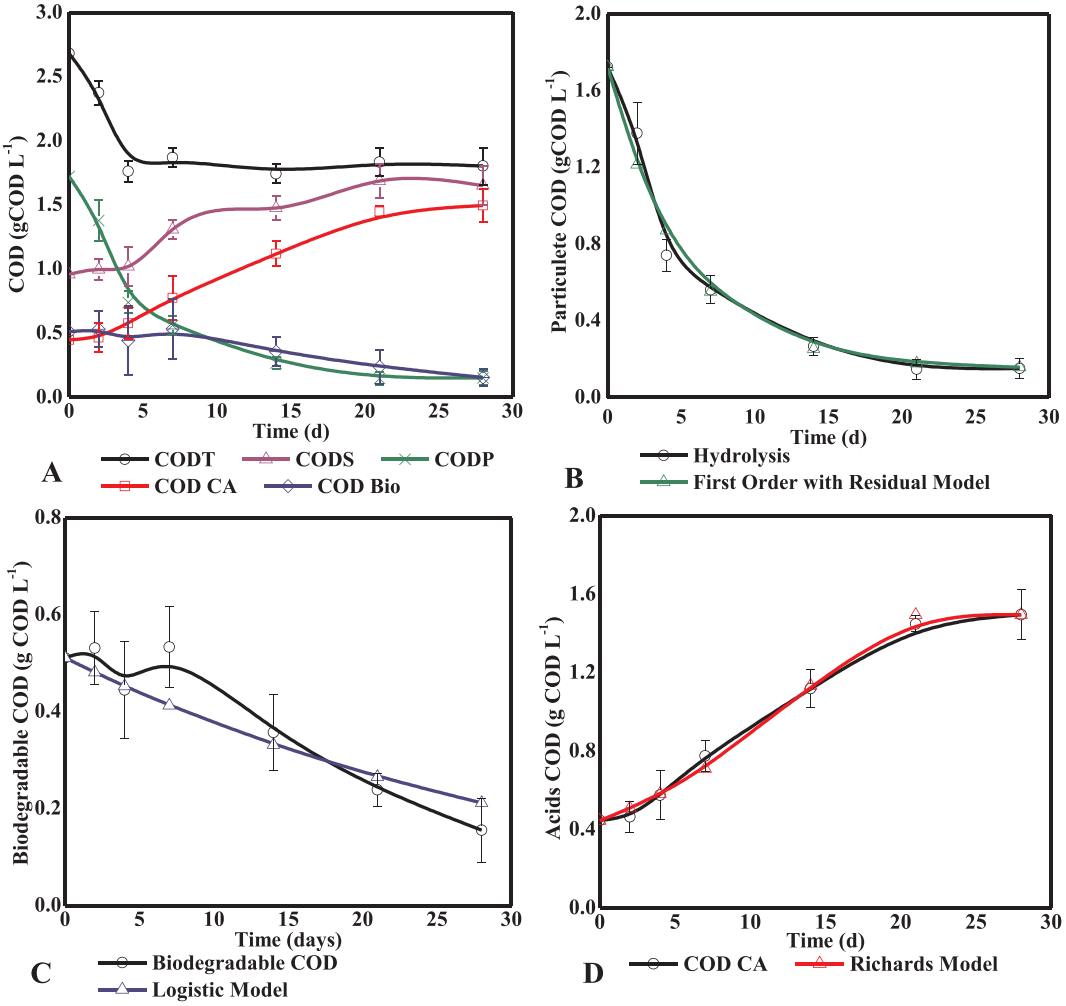

Fig. 1. Profiles of organic matter concentration (hydrolysis, consumption and CA production) during the CAPP assays. (A) Profiles of organic matter concentration. (B) Kinetic modeling of hydrolysis of particulate organic matter (First-order with residual model). (C) Kinetic modeling of the biodegradable organic matter consumption (Logistic model). (D) Kinetic modeling of COD production in the form of carboxylic acids (Richards model).

according to Eq. (9).

$$AIC = N.\ ln\left(\frac{SS}{N}\right) + 2k \tag{9}$$

where: AIC is the Akaike Information Criterion (dimensionless); N is the number of observations of experimental data; SS is the square sum of the residuals and k is the number of model parameters.

3. Results and discussion

3.1. Organic matter fractions and yields

On average, 40 ± 5% of the applied organic matter (558.4 $mgCOD_A$) was converted to CA (224.9 ± 28.1 $mgCOD_{CA}$), representing a yield of 0.33 mg $mgCOD_A^{-1}$ ($Y2_{CA}$) which is equivalent to 0.40 mgCOD $mgCOD_A^{-1}$ ($Y1_{CA}$). The main CA formed were HAc and HBu with a selectivity of 75% and 13%, respectively (Table 3). On average, 80% of the COD converted to CA was directed to the formation of HAc and HBu, which are the main electron acceptors to be converted to HCa and HCap in the BCCEP (Angenent et al., 2016). Even without the external addition of electron donors, such as ethanol (EtOH) and lactic acid (HLa), to favor the BCCEP, HCa was formed even at low concentrations (49 ± 5 mg L^{-1}) and selectivity (4 ± 0%) (Table 3).

As no external electron donor was added, it is believed that EtOH and H_2, formed in the metabolic pathways of organic matter degradation, were the major contributors to the production of MCCAs (Ding et al., 2010). Under standard conditions of temperature and pressure (STP), HCa formation is thermodynamically less favorable when using EtOH as an electron donor compared to H_2, due to the higher H_2 diffusion through the cytoplasmic membrane (Seedorf et al., 2008). This latter metabolic process occurs when there are low concentrations of EtOH and high concentrations of SCCAs, such as HAc and HBu (Steinbusch et al., 2011; Zhang et al., 2013). However, H_2 as an electron donor does not promote high HCa productivity, because in this process there is low production of reducing coefficients (important for BCCEP electron flux), unlike when EtOH is an electron donor (Ding et al., 2010).

According to Vasudevan et al. (2014), the production of HCa in mixed cultures may require the addition of an inorganic carbon source, especially when EtOH and HAc are used as substrates. This is because *Clostridium kluyveri*, one of the most important microorganisms for biological production of HCa (Kannengiesser et al., 2016), requires an inorganic carbon source (CO_2) for protein synthesis (Roghair et al., 2018). Studies indicate that during the production of HCa, about 30% of carbon assimilated to cell biomass is derived from CO_2, while 70% is derived from organic carbon (Jungermann et al., 1968). However, in acidogenic reactors fed with complex substrates such as SW, inorganic carbon supplementation is not required due to the internal production of CO_2 during the hydrolytic-acidogenic stage of organic matter (Cavalcante et al., 2017), as noted by the predominance of CO_2 in the

Table 4
Kinetic parameters estimated by the modeling of organic matter conversion bioprocesses.

Model	Parameters		Model	Parameters	
Hydrolysis of Particulate Organic Matter					
First-order	k_H (d^{-1})	0.16 ± 0.02	First-order with residual	Cr (gCOD L^{-1})	0.15 ± 0.05
	R^2	0.967		k_H (d^{-1})	0.20 ± 0.03
	AIC	−29.691		R^2	0.981
				AIC	−33.360
Consumption of Biodegradable Organic Matter					
First-order	k_B (d^{-1})	0.03 ± 0.01	First-order with residual	Cr (gCOD L^{-1})	0.16 ± 0.07
	R^2	0.836		k_B (d^{-1})	0.05 ± 0.01
	AIC	−38.216		R^2	0.787
				AIC	−36.386
Monod with growth	Ks (gCOD L^{-1})	2.75 ± 0.60	Logistic	k_L (L $gCOD^{-1}$ d^{-1})	0.007 ± 0.003
	X (gSSV L^{-1})	4.34 ± 0.50		k_B (d^{-1})	0.03 ± 0.01
	$\mu_{máx}$ (d^{-1})	0.02 ± 0.01		R^2	0.842
	k_L (L $gCOD^{-1}$ d^{-1})	0.008 ± 0.004		AIC	−38.445
	k_B (d^{-1})	0.03 ± 0.02			
	R^2	0.876			
	AIC	−36.167			
Production of Carboxylic Acids					
First-order	k_{AC} (d^{-1})	0.12 ± 0.03	Second-order	k_{AC}" (L $gCOD^{-1}$ d^{-1})	0.15 ± 0.04
	R^2	0.799		R^2	0.734
	AIC	−21.473		AIC	−19.503
Fitzhugh	k_{AC} (d^{-1})	0.10 ± 0.02	Mono molecular	k_{AC} (d^{-1})	0.12 ± 0.03
	n	0.81 ± 0.19		λ (d)	0.00 ± 0.00
	R^2	0.805		R^2	0.799
	AIC	−19.696		AIC	−19.473
Modified Gompertz	μ_m (gCOD L^{-1} d^{-1})	0.11 ± 0.03	Logistic	μ_m (gCOD L^{-1} d^{-1})	0.10 ± 0.03
	λ (d)	0.00 ± 0.00		λ (d)	0.00 ± 0.00
	R^2	0.826		R^2	0.869
	AIC	−20.471		AIC	−22.470
Transference	μ_m (gCOD L^{-1} d^{-1})	0.18 ± 0.03	Richards	v	18.64 ± 0.40
	λ (d)	0.00 ± 0.00		μ_m (gCOD L^{-1} d^{-1})	0.09 ± 0.04
	R^2	0.799		λ (d)	0.00 ± 1.5
	AIC	−19.473		R^2	0.993
				AIC	−41.072

k_H: hydrolysis rate constant; k_B: soluble substrate degradation rate constant; C_r: residual COD concentration; K_S: saturation constant/Monod constant; X: final biomass concentration; μ_{max}: maximum microbial growth rate; k_L: Logistic model constant; k_{CA}: first-order CA production rate constant, k_{CA}": second-order CA production rate constant; n: form constant; λ: lag phase time; μ_m: maximum CA productivity; R^2: coefficient of determination; AIC: Akaike Information Criteria.

biogas formed in the bioreactors (data not shown).

The production of acids in fermentative systems depends on many factors such as temperature, pH, type of inoculum, ways to extract the formed products, among others, which influence the metabolic pathways (Atasoy et al., 2018). For instance, pyruvate can be converted into a wide range of products, such as HAc, HPr, HBu, EtOH, H_2 and CO_2 (Chen et al., 2013). Therefore, the selectivity of CA production will depend on the proportions of pyruvate directed to each acidogenic metabolic pathway (Jiang et al., 2013).

HAc and EtOH are the main products of acidogenic fermentation of organic matter, formed mainly in the acetate-ethanol fermentation pathway, and generally react in fermentation to produce H_2 (Zhang et al., 2017). HAc can be obtained from pyruvate via the acetyl-CoA pathway, but can also be generated from the syntrophic oxidation of EtOH or longer-chain carboxylic acids such as HPr and HBu (Müller et al., 2010), as well as from the homoacetogenesis pathway.

The high selectivity of HAc (75%) can be due to the mesophilic temperature of the experiment (35 °C) since many studies indicate that there is a prevalence of HAc and HPr formation at mesophilic temperatures (35 to 45 °C), while HBu selectivity increases at thermophilic temperatures (55 °C) (Jiang et al., 2013).

However, in our case, because HPr presented a reduction in the concentration since the beginning of the batch, the yield and maximum productivity for this CA were not calculated. However, the concentration of HPr (mgCOD) at the end of the batch test was considered for calculations of total CA production yield ($Y1_{CA}$ and $Y2_{CA}$). The bioconversion of HPr to HAc by syntrophic oxidation and the transformation of HPr to HVa by BCCEP are likely the main factors that may have contributed to the higher consumption of this CA (Müller et al., 2010; Zhou et al., 2018). HPr consumption was also reported by Yin et al. (2016), who evaluated the production of CA in batch reactors, using peptone as substrate and a microbial anaerobic consortium collected from a brewery wastewater treatment.

pH is considered a critical factor controlling CA production during acidogenic fermentation because it affects the displacement of the acidogenic metabolic pathways (Zhou et al., 2018). Studies indicate that under neutral conditions most of the protein in the substrate can be transformed into ammoniacal nitrogen which acts as an additional buffer agent to the acidified fermentation systems (Zhang et al., 2005; Plácido and Zhang, 2018). According to Cavalcante et al. (2017), the pH near neutrality favors the metabolism of *C. kluyveri*, being an important operational parameter when aiming at the production of HCa. Thus, likely the use of pH close to 7.0 may have contributed to the acidogenic process and synthesis of HCa from SW fermentation.

3.2. Kinetic modeling

As can be seen in Fig. 1A, soluble organic matter was made available gradually by the hydrolysis process of particulate organic matter. From the seventh day, with the decrease of hydrolysis rate, there was a predominance of bioconversion of soluble organic matter in CA, indicated by the reduction of the biodegradable COD fraction (soluble COD not referring to CA) and the increasing gCOD values referring to CA.

According to Table 4, the value of the soluble substrate degradation rate constant (Logistic model: $k_B = 0.03 \pm 0.01$ d^{-1}) was lower than

Table 5
Mean values of kinetic parameters estimated by modeling the production of carboxylic acids in the acidogenic fermentation of SW.

Modelo	Parâmetros	HAc	HBu	HIva	HVa	HCa
First-order	k_{AC} (d^{-1})	0.125	0.127	0.130	0.064	0.057
	R^2	0.994	0.965	0.920	0.883	0.839
	AIC	−51.560	−62.804	−67.276	−81.717	−65.590
Second-order	k_{AC}" (L g^{-1} d^{-1})	0.283	1.627	3.764	4.891	1.609
	R^2	0.938	0.885	0.821	0.783	0.733
	AIC	−35.388	−54.385	−61.599	−77.431	−62.080
Fitzhugh	k_{AC} (d^{-1})	0.122	0.151	0.169	0.160	0.202
	n	0.963	1.245	1.444	3.986	9.708
	R^2	0.994	0.969	0.928	0.981	0.998
	AIC	−49.687	−61.534	−66.002	−92.442	−94.571
Monomolecular	k_{AC} (d^{-1})	0.125	0.130	0.133	0.075	0.069
	λ (d)	0.000	0.172	0.113	1.779	2.180
	R^2	0.994	0.966	0.921	0.920	0.887
	AIC	−49.560	−60.958	−65.304	−82.431	−66.067
Modified Gompertz	μ_m (g L^{-1} d^{-1})	0.066	0.011	0.005	0.001	0.004
	λ (d)	0.000	0.000	0.000	4.210	6.905
	R^2	0.973	0.962	0.942	0.977	0.998
	AIC	−39.120	−60.116	−67.446	−91.181	−93.690
Logistic	μ_m (g L^{-1} d^{-1})	0.061	0.010	0.005	0.001	0.004
	λ (d)	0.000	0.000	0.439	5.259	7.758
	R^2	0.956	0.950	0.950	0.958	0.990
	AIC	−35.766	−58.290	−68.465	−86.948	−83.096
Transference	μ_m (g L^{-1} d^{-1})	0.100	0.018	0.008	0.001	0.003
	λ (d)	0.000	0.172	0.113	1.779	2.180
	R^2	0.994	0.966	0.921	0.920	0.887
	AIC	−49.560	−60.958	−65.304	−82.431	−66.067
Richards	*v*	0.000	0.000	0.000	0.001	0.000
	μ_m (g L^{-1} d^{-1})	0.000	0.000	0.000	0.000	0.000
	λ (d)	0.000	0.000	0.468	6.321	10.132
	R^2	0.973	0.962	0.930	0.947	0.811
	AIC	−37.119	−58.115	−64.138	−83.345	−60.490

k_{CA}: first-order CA production rate constant, k_{CA}": second-order CA production rate constant; n: form constant; λ: lag phase time; μ_m: maximum CA productivity; R^2: coefficient of determination; AIC: Akaike Information Criteria.

the hydrolysis rate constant (First-order residual model: $k_H = 0.20 \pm 0.03\ d^{-1}$), values estimated by the models that obtained the best fit in the kinetic modeling of these biological processes. As $k_H > k_B$, the rate of degradation of particulate organic matter was higher than the rate of consumption of soluble organic matter (biodegradable COD). This was because the particulate COD concentration (1.72 gCOD L^{-1}) was higher than the biodegradable COD concentration (0.51 gCOD L^{-1}) at the beginning of the experiment.

The First-order with residual kinetic model best described the hydrolysis process of particulate organic matter (Fig. 1B), with a high R^2 (0.981) and low AIC (−33.36) (Table 4). This model proved to be ideal for mathematical simulation of the hydrolysis process of the particulate organic matter of SW in methanogenic inhibited systems. No kinetic model applied suited the consumption profile of soluble biodegradable organic matter (Fig. 1C). This is because the models used do not consider the increases of soluble organic matter concentration that was caused by hydrolysis. The Logistic model was the one with the lowest AIC (−38,445). However, there is a low correlation between the experimental values and those predicted by this model (Fig. 1C), as indicated by the low R^2 value (0.842) (Table 4). The Logistic model constant ($k_L = 0.007 \pm 0.003$ L $gCOD^{-1}$ d^{-1}) can be defined as the ratio between the maximum growth rate and the saturation constant ($\mu_{máx}$/Ks). The higher k_L the greater the affinity of microorganisms for the substrate (Phukoetphim et al., 2017). As $k_H > k_B$ and $k_H > k_L$, it is understood that the hydrolysis process influenced the low values of k_L and k_B obtained in relation to the k_H value, limiting the rate of utilization of soluble substrate by microorganisms.

The kinetic modeling of COD_{CA} production was best described by the Richards model ($R^2 = 0.993$ and AIC = −41.072). The dimensionless factor *v* present in the equation of this model allows the curve inflection point to occur at any point between the minimum and maximum production asymptote, leading to a better fit of the model to the experimental curves. This does not occur for modeling performed with the Modified Gompertz and Logistic models because they have a fixed inflection point, and the rest of the curve is modeled according to the location of this point, making it difficult to adjust to experimental curves (Ware and Power, 2017).

It can be seen that CA production from SW in mixed culture follows a logistic growth kinetics, as evidenced by the higher R^2 values and lower AIC values from the Richards model ($R^2 = 0.993$ and AIC = −41.072) and from the Logistic model ($R^2 = 0.869$ and AIC = −22.470) in relation to exponential growth models such as the First-Order model ($R^2 = 0.799$ and AIC = −21.473), the Second-order model ($R^2 = 0.734$ and AIC = −19.503), and the Monomolecular model ($R^2 = 0.799$ and AIC = −19.473). Thus, kinetic models that describe logistic functions, such as Richards and Logistic models, are the most suitable for satisfactorily describing CA production from SW. This is because the CA production curve is characterized by an elongated S-shape (Fig. 1D).

According to Labatut et al. (2011), the production curve shape reflects the biodegradability characteristics of the substrates, the kinetics of the biological processes and the performance of the microorganisms involved. The sigmoidal shape curves consist of three phases: the slow production phase or the acclimatization of the microorganisms (lag phase), the fast production phase (exponential phase) with higher substrate consumption and biomass growth and the production stabilization phase, where the production rate decreases and eventually reaches zero (Ware and Power, 2017). This type of curve is common for substrates that have high concentrations of complex organic compounds, such as fats or lignocellulose, and which have the hydrolysis step as limiting anaerobic process (Labatut et al., 2011). Therefore, an elongated S-shaped curve indicates gradual availability of soluble organic matter and also a more gradual production of CA over time.

Hydrolysis was the limiting step of SW acidogenic fermentation

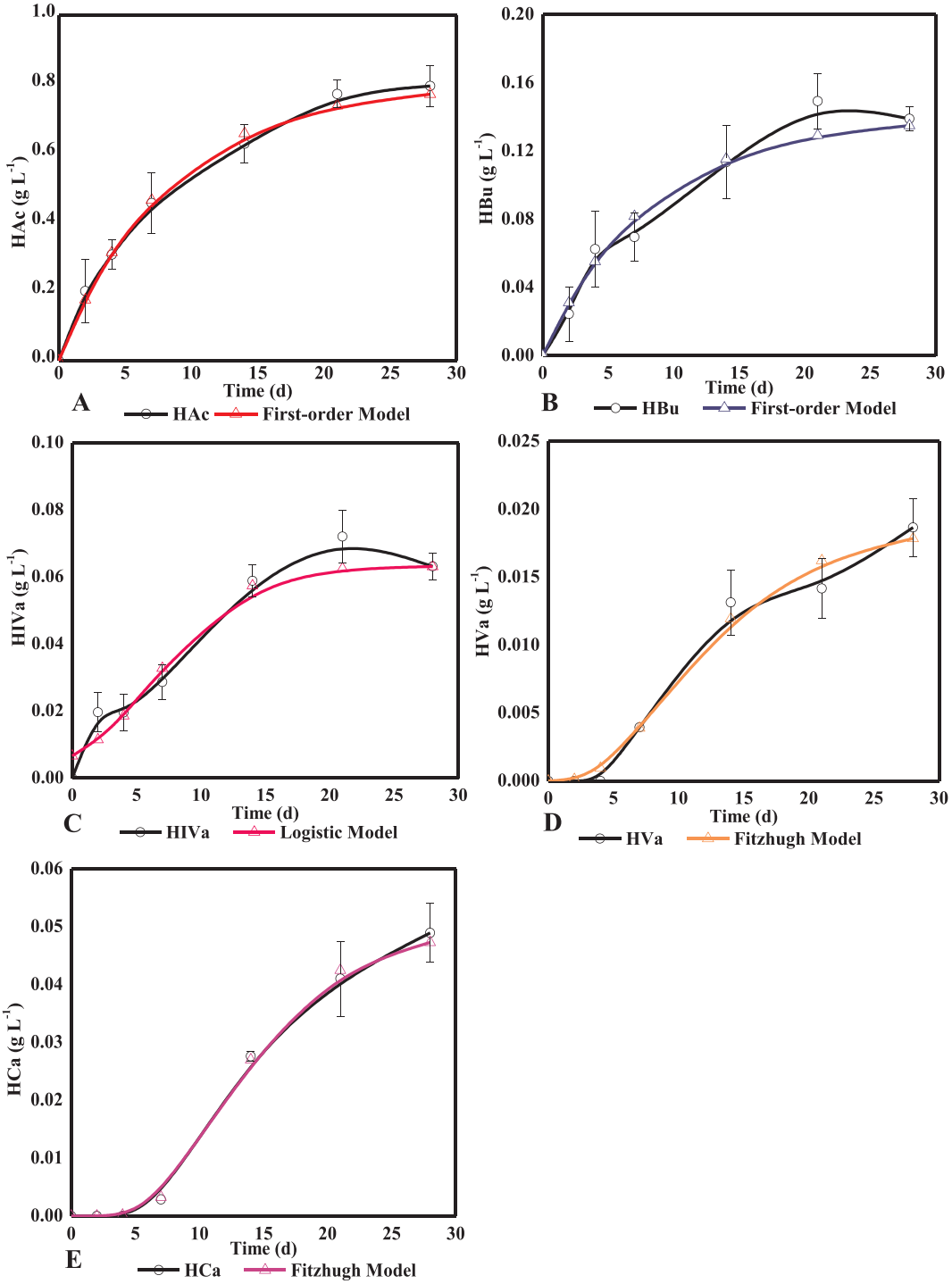

Fig. 2. Kinetic modeling of the production of carboxylic acids. (A) HAc. (B) HBu. (C) HIVa. (D) HVa. (E) HCa.

(Kim et al., 2005) due to the high concentration of particulate organic material at the beginning of the experiment (COD_P/COD_A = 0.77), once that it took more than twenty days for the particulate COD consumption to stabilize (Fig. 1B) and fourteen days to produce 60% of the acids formed (134.9 $mgCOD_{CA}$) (Fig. 1D). In this context, improved hydrolysis rate could increase the availability of soluble organic matter faster. Thus, techniques for accelerating the hydrolysis process, such as the use of thermophilic temperatures, microaeration, among others, can be investigated to maximize the yield of CA production (Fdez-Güelfo et al., 2011).

According to Ding et al. (2017), SW is a liquid organic waste with high content of particulate organic matter because it is formed mainly by proteins and lipids from animal excrements and undigested food waste. In our case, the characterization showed high concentrations of suspended solids (8,602 mg L^{-1}), chemical oxygen demand (18,707 mgO_2 L^{-1}), total biochemical oxygen demand (9,979 mgO_2 L^{-1}), total nitrogen (361 mg N L^{-1}) and total phosphorus (150 mg P L^{-1}).

Despite the gradual availability of soluble organic matter, the Modified Gompertz, Monomolecular, Transference and Logistic kinetic models estimated lag phase time equal to zero (λ = 0 d) and the form factor (n = 0.81) of the Fitzhugh model was lower than unity, indicating good microbial affinity by the soluble substrate and the

absence of lag phase in relation to CA production from SW (Lima et al., 2018).

The models with the best performance in simulating CA production were: First-order model for HAc and HBu, Logistic model for HIVa and Fitzhugh model for HVa and HCa (Table 5 and Fig. 2). These models indicated that the highest first-order production rate constant was for HCa (k_{AC}' = 0.202 d^{-1}) and the lowest for HAc (k_{AC}' = 0.125 d^{-1}), although the final concentration, maximum productivity and selectivity for HAc were much higher (Table 3). So the first-order production rate constants provided by the models must be interpreted carefully and an integrated analysis with other parameters must be performed.

Therefore, the maximum acid yield (μ_m) estimated by the models that best fit the experimental data was 100 mg L^{-1} d^{-1} (Transference model); 18 mg L^{-1} d^{-1} (Transference model); 5 mg L^{-1} d^{-1} (Modified Gompertz model); 1 mg L^{-1} d^{-1} (Modified Gompertz model) and 4 mg L^{-1} d^{-1} (Modified Gompertz model) for HAc, HBu, HIVa, HVa and HCa, respectively. These μ_m values are very close to those calculated directly with the concentration data obtained on the collection days (Table 5), indicating that the applied kinetic models were able to satisfactorily estimate this parameter.

Regarding lag time (λ), the models indicated a time of less than one day to start HAc, HBu and HIVa production. However, the λ values for HVa and HCa were 4.2 and 6.9 d, respectively, according to the Modified Gompertz model (Table 5 and Fig. 2). The kinetic modeling of HPr production was not presented because the consumption of this CA was higher than its production, probably for HAc production. Thus, no production model could describe the behavior of HPr concentration variations during the experimental period.

4. Conclusions

The potential of anaerobic carboxylic acids (CA) production from swine wastewater was assessed, as well as modeling studies of the acidogenic process on methanogenic inhibited systems were performed. Hydrolysis was the main limiting step of CA production from SW, once that it took more than twenty days for the particulate COD consumption to stabilize and fourteen days to produce 60% of the acids formed. The main CA formed were HAc and HBu and a yield 0.33 mg $mgCOD_A^{-1}$, corresponding to 0.40 mgCOD $mgCOD_A^{-1}$, was obtained. Kinetic models describing logistic growth functions were best suited to simulate CA production.

Declaration of Competing Interest

The authors declare that they have no known competing financial interests or personal relationships that could have appeared to influence the work reported in this paper.

Acknowledgements

The authors would like to acknowledge the support obtained from the following Brazilian institutions: Conselho Nacional de Desenvolvimento Científico e Tecnológico – CNPq; Coordenação de Aperfeiçoamento de Pessoal de Nível Superior – CAPES; Fundação de Amparo à Pesquisa do Estado de Minas Gerais – FAPEMIG; Instituto Nacional de Ciência e Tecnologia em Estações Sustentáveis de Tratamento de Esgoto – INCT ETEs Sustentáveis (INCT Sustainable Sewage Treatment Plants), and Empresa Brasileira de Pesquisa Agropecuária – EMBRAPA.

Appendix A. Supplementary data

Supplementary data to this article can be found online at https://doi.org/10.1016/j.biortech.2019.122520.

References

Angenent, L.T., Richter, H., Buckel, W., Spirito, C.M., Steinbusch, K.J.J., Plugge, C.M., Strik, D.P.B.T.B., Grootscholten, T.I.M., Buisman, C.J.N., Hamelers, H.V.M., 2016. Chain elongation with reactor microbiomes: open-culture biotechnology to produce biochemicals. Environ. Sci. Technol. 50, 2796–2810.

APHA (American Public Health Association), American Water Works Association, Water Environment Federation, 2012. Standard Methods for the Examination of Water and Wastewater. 22th ed. American Public Health Association (APHA), American Water Works Association and Water Environment Federation, Washington, DC.

Atasoy, M., Owusu-Agyeman, I., Plaza, E., Cetecioglu, Z., 2018. Bio-based volatile fatty acid production and recovery from waste streams: Current status and future challenges. Bioresour. Technol. 268, 773–786.

Cavalcante, W.A., Leitão, R.C., Gehring, T.A., Angenent, L.T., Santaella, S.T., 2017. Anaerobic fermentation for n-caproic acid production: a review. Process Biochem. 54, 106–119.

Chen, Y., Luo, J., Yan, Y., Feng, L., 2013. Enhanced production of short-chain fatty acid by co-fermentation of waste activated sludge and kitchen waste under alkaline conditions and its application to microbial fuel cells. Appl. Energy 102, 1197–1204.

Cheng, D., Ngo, H.H., Guo, W.S., Chang, S.W., Kumar, S.M., Du, B., Wei, Q., Wei, D., 2018. Problematic effects of antibiotics on anaerobic treatment processes in swine wastewater. Bioresour. Technol. 263, 642–653.

Cheng, D.L., Ngo, H.H., Guo, W.S., Chang, S.W., Nguyen, D.D., Kumar, S.M., 2019. Microalgae biomass from swine wastewater and its conversion to bioenergy. Bioresour. Technol. 275, 109–122.

Dams, R.I., Viana, M.B., Guilherme, A.A., Silva, C.M., Dos Santos, A.B., Angenent, L.T., Santaella, S.T., Leitão, R.C., 2018. Production of medium-chain carboxylic acids by anaerobic fermentation of glycerol using a bioaugmented open culture. Biomass Bioenergy 118, 1–7.

Ding, H.-B., Tan, G.-Y.A., Wang, J.-Y., 2010. Caproate formation in mixed-culture fermentative hydrogen production. Bioresour. Technol. 101, 9550–9559.

Ding, W., Cheng, S., Yu, L., Huang, H., 2017. Effective swine wastewater treatment by combining microbial fuel cells with flocculation. Chemosphere 182, 567–573.

Ebrahimi, A., Hashemi, H., Eslami, H., Fallahzadeh, R.A., Khosravi, R., Askari, R., Ghahramani, E., 2018. Kinetics of biogas production and chemical oxygen demand removal from compost leachate in an anaerobic migrating blanket reactor. J. Environ. Manage. 206, 707–714.

Fang, W., Zhang, X., Zhang, P., Wan, J., Guo, H., Ghasimi, D.S.M., Morera, X.C., Zhang, T., 2020... Overview of key operation factors and strategies for improving fermentative volatile fatty acid production and product regulation from sewage sludge. J. Environ. Sci. 87, 93–111.

FAO. Food and Agriculture Organization of the United Nations. 2019. Meat Market Review: Overview of global meat market developments in 2018. Food and Agriculture Organization of the United States (FAO), Rome, March 2019. < http://www.fao.org/3/ca3880en/ca3880en.pdf > (Accessed on August 24 2019).

Fdez-Güelfo, L.A., Álvarez-Gallego, C., Sales, D., Romero, L.I., 2011. The use of thermochemical and biological pretreatments to enhance organic matter hydrolysis and solubilization from organic fraction of municipal solid waste (OFMSW). Chem. Eng. J. 168, 249–254.

García, D., Posadas, E., Grajeda, C., Blanco, S., Martínez-Páramo, S., Acién, G., García-Encina, P., Bolado, S., Muñoz, R., 2017. Comparative evaluation of piggery wastewater treatment in algal-bacterial photobioreactors under indoor and outdoor conditions. Bioresour. Technol. 245, 483–490.

Groen, E.A., van Zanten, H.H.E., Heijungs, R., Bokkers, E.A.M., de Boer, I.J.M., 2016. Sensitivity analysis of greenhouse gas emissions from a pork production chain. J. Clean. Prod. 129, 202–211.

Han, W., He, P., Shao, L., Lü, F., 2019. Road to full bioconversion of biowaste to biochemicals centering on chain elongation: A mini review. J. Environ. Sci. 86, 50–64.

Huang, H., Zhang, D., Li, J., Guo, G., Tang, S., 2017. Phosphate recovery from swine wastewater using plant ash in chemical crystallization. J. Clean. Prod. 168, 338–345.

Huang, H., Zhang, P., Zhang, Z., Liu, J., Xiao, J., Gao, F., 2016. Simultaneous removal of ammonia nitrogen and recovery of phosphate from swine wastewater by struvite electrochemical precipitation and recycling technology. J. Clean. Prod. 127, 302–310.

Jiang, J., Zhang, Y., Li, K., Wang, Q., Gong, C., Li, M., 2013. Volatile fatty acids production from food waste: Effects of pH, temperature, and organic loading rate. Bioresour. Technol. 143, 525–530.

Jungermann, K., Thauer, R.K., Decker, K., 1968. The synthesis of one-carbon units from CO_2 in Clostridium kluyveri. Eur. J. Biochem. 3, 351–359.

Kannengiesser, J., Sakaguchi-Söder, K., Mrukwia, T., Jager, J., Schebek, L., 2016. Extraction of medium chain fatty acids from organic municipal waste and subsequent production of bio-based fuels. Waste Manage. 47, 78–83.

Kim, H.J., Choi, Y.G., Kim, D.Y., Kim, D.H., Chung, T.H., 2005. Effect of pretreatment on acid fermentation of organic solid waste. Water Sci. Technol. 52, 153–160.

Kwon, G., Kang, J., Nam, J.H., Kim, Y.O., Jahng, D., 2018. Recovery of ammonia through struvite production using anaerobic digestate of piggery wastewater and leachate of sewage sludge ash. Environ. Technol. 39, 831–842.

Labatut, R.A., Angenent, L.T., Scott, N.R., 2011. Biochemical methane potential and biodegradability of complex organic substrates. Bioresour. Technol. 102, 2255–2264.

Leite, L. de S., Hoffmann, M.T., Daniel, L.A., 2019. Microalgae cultivation for municipal and piggery wastewater treatment in Brazil. J. Water Process Eng. 31 100821.

Lima, D.R.S., Adame, O.F.H., Baêta, B.E.L., Gurgel, L.V.A., De Aquino, A.F., 2018. Influence of different thermal pretreatments and inoculum selection on the biomethanation of sugarcane bagasse by solid-state anaerobic digestion: a kinetic analysis. Ind. Crops Prod. 111, 684–693.

Membere, E., Sallis, P., 2018. Effect of temperature on kinetics of biogas production from macroalgae. Bioresour. Technol. 263, 410–417.
Moscoviz, R., Trably, E., Berneta, N., Carrèrea, H., 2018. The environmental biorefinery: state-of-the-art on the production of hydrogen and value-added biomolecules in mixed-culture fermentation. Green Chem. 20, 3159–3179.
Müller, N., Worm, P., Schink, B., Stams, A.J., Plugge, C.M., 2010. Syntrophic butyrate and propionate oxidation processes: from genomes to reaction mechanisms. Environ. Microbiol. Rep. 2, 489–499.
Nagarajan, D., Kusmayadi, A., Yen, H.-W., Dong, C.-D., Lee, D.-J., Chang, J.-S., 2019. Current advances in biological swine wastewater treatment using microalgae-based processes. Bioresour. Technol. 289, 121718.
Phukoetphim, N., Salakkam, A., Laopaiboon, P., Laopaiboon, L., 2017. Kinetic models for batch ethanol production from sweet sorghum juice under normal and high gravity fermentations: Logistic and modified Gompertz models. J. Biotechnol. 243, 69–75.
Plácido, J., Zhang, Y., 2018. Production of volatile fatty acids from slaughterhouse blood by mixed-culture fermentation. Biomass Convers. Biorefinery 8, 621–634.
Roghair, M., Hoogstad, T., Strik, D.P.B.T.B., Plugge, C.M., Timmers, P.H.A., Weusthuis, R.A., Bruins, M.E., Buisman, C.J.N., 2018. Controlling ethanol use in chain elongation by CO_2 loading rate. Environ. Sci. Technol. 52, 1496–1505.
Seedorf, H., Fricke, W.F., Veith, B., Brüggemann, H., Liesegang, H., Strittmatter, A., Miethke, M., Buckel, W., Hinderberger, J., Li, F., Hagemeier, C., Thauer, R.K., Gottschalk, G., 2008. The genome of Clostridium kluyveri, a strict anaerobe with unique metabolic features. PNAS 105, 2128–2133.
Steinbusch, K.J.J., Hamelers, H.V.M., Plugge, C.M., Buisman, C.J.N., 2011. Biological formation of caproate and caprylate from acetate: fuel and chemical production from low grade biomass. Energy Environ. Sci. 4, 216–224.
Sun, C., Cao, W., Liu, R., 2015. Kinetics of methane production from swine manure and buffalo manure. Appl. Biochem. Biotechnol. 177, 985–995.
Vasudevan, D., Richter, H., Angenent, L.T., 2014. Upgrading dilute ethanol from syngas fermentation to n-caproate with reactor microbiomes. Bioresour. Technol. 151, 378–382.
Viana, M.B., Dams, R.I., Pinheiro, B.M., Leitão, R.C., Santaella, S.T., Dos Santos, A.B., 2019. The source of inoculum and the method of methanogenesis inhibition can affect biological hydrogen production from crude glycerol. Bioenergy Res. 12, 1–10.
Wagner, R.C., Regan, J.M., Oh, S.-E., Zuo, Y., Logan, B.E., 2009. Hydrogen and methane production from swine wastewater using microbial electrolysis cells. Water Res. 43, 1480–1488.
Ware, A., Power, N., 2017. Modelling methane production kinetics of complex poultry slaughterhouse wastes using sigmoidal growth function. Renew. Energy. 104, 50–59.
Xu, Z., Song, X., Li, Y., Li, G., Luo, W., 2019. Removal of antibiotics by sequencing-batch membrane bioreactor for swine wastewater treatment. Sci. Total Environ. 684, 23–30.
Yang, H., Deng, L., Liu, G., Yang, D., Liu, Y., Chen, Z., 2016. A model for methane production in anaerobic digestion of swine wastewater. Water Res. 102, 464–474.
Yin, J., Yu, X., Wang, K., Shen, D., 2016. Acidogenic fermentation of the main substrates of food waste to produce volatile fatty acids. Int. J. Hydrogen Energy 41, 21713–21720.
Yin, Y., Zhang, Y., Karakashev, D.B., Wang, J., Angelidaki, I., 2017. Biological caproate production by Clostridium kluyveri from ethanol and acetate as carbon sources. Bioresour. Technol. 241, 638–644.
Zhang, B., Zhang, L.L., Zhang, S.C., Shi, H., Cai, W.M., 2005. The influence of pH hydrolysis and acidogenesis of kitchen wastes in two-phase anaerobic digestion. Environ. Technol. 26, 329–339.
Zhang, F., Ding, J., Zhang, Y., Chen, M., Ding, Z.W., van Loosdrecht, M.C., Zeng, R.J., 2013. Fatty acids production from hydrogen and carbon dioxide by mixed culture in the membrane biofilm reactor. Water Res. 47, 6122–6129.
Zhang, S., Liu, M., Chen, Y., Pan, Y.-T., 2017. Achieving ethanol-type fermentation for hydrogen production in a granular sludge system by aeration. Bioresour. Technol. 224, 349–357.
Zhou, M., Yan, B., Wong, J.W.C., Zhang, Y., 2018. Enhanced volatile fatty acids production from anaerobic fermentation of food waste: a mini-review focusing on acidogenic metabolic pathways. Bioresour. Technol. 248, 68–78.